# Predicting the impact of non-pharmaceutical interventions against COVID-19 on *Mycoplasma pneumoniae* in the United States

Sang Woo Park[1,2,*], Brooklyn Noble[3], Emily Howerton[1], Bjarke F Nielsen[4], Sarah Lentz[3], Lilliam Ambroggio[5], Samuel Dominguez[6], Kevin Messacar[6], Bryan T Grenfell[1]

**1** Department of Ecology and Evolutionary Biology, Princeton University, Princeton, NJ, USA
**2** Department of Ecology and Evolution, University of Chicago, Chicago, IL, USA
**3** bioMérieux, Salt Lake City, Utah, USA
**1** Department of Ecology and Evolutionary Biology, Princeton University, Princeton, NJ, USA
**4** High Meadows Environmental Institute, Princeton University, Princeton, New Jersey, USA
**5** Department of Pediatrics, Sections of Emergency Medicine and Hospital Medicine, University of Colorado School of Medicine and Children's Hospital Colorado, Aurora, CO, USA
**6** Department of Pediatrics, Section of Infectious Diseases, University of Colorado School of Medicine and Children's Hospital Colorado, Aurora, CO, USA

*Corresponding author: swp2@uchicago.edu

## Abstract

The introduction of non-pharmaceutical interventions (NPIs) against COVID-19 disrupted circulation of many respiratory pathogens and eventually caused large, delayed outbreaks, owing to the build up of the susceptible pool during the intervention period. In contrast to other common respiratory pathogens that re-emerged soon after the NPIs were lifted, longer delays ($> 3$ years) in the outbreaks of *Mycoplasma pneumoniae* (Mp), a bacterium commonly responsible for respiratory infections and pneumonia, have been reported in Europe and Asia. As Mp cases are continuing to increase in the US, predicting the size of an imminent outbreak is timely for public health agencies and decision makers. Here, we use simple mathematical models to provide robust predictions about a large Mp outbreak ongoing in the US. Our model further illustrates that NPIs and waning immunity are important factors in driving long delays in epidemic resurgence.

# 1 Introduction

*Mycoplasma pneumoniae* (Mp) is the most commonly detected bacterium for lower tract respiratory infections in children and adults (Waites and Talkington, 2004; Jain et al., 2015,?; Bajantri et al., 2018). Mp pneumonia can affect a patient for a long period due to its long incubation period and long prodromal duration of symptoms, especially among children and high risk individuals. For instance, outbreaks in schools have resulted in increased hospitalization, ventilator-associated pneumonia, severe extrapulmonary disease (e.g. Stevens-Johnson syndrome) and have been shown to last for several months (Walter et al., 2008; Olson et al., 2015). Increasing levels of macrolide-resistant Mp strains further highlight the importance of appropriate diagnosis and treatment (Pereyre et al., 2016).

Multiannual cycles in Mp outbreak patterns have been observed in many countries, with large outbreaks occurring every 3–7 years (Kim et al., 2009; Brown et al., 2016). Several potential mechanisms have been proposed to explain the observed epidemic cycles, including waning immunity (Omori et al., 2015) and strain dynamics (Kenri et al., 2008; Zhang et al., 2019). More parsimoniously, multiennial epidemic dynamics can also arise from simple, seasonally-forced immunizing epidemic dynamics, especially given low transmission rates (Earn et al., 2000; Keeling et al., 2001).

Along with other endemic viruses and bacteria, the circulation of Mp was disrupted in 2020 due to non-pharmaceutical interventions (NPIs) that were introduced to prevent the transmission of SARS-CoV-2 (Boyanton Jr et al., 2024). The disruption of the expected epidemiological curve adds challenges to predicting future Mp outbreaks. In contrast to other common respiratory pathogens that re-emerged within a year after NPIs were lifted, the re-emergence of Mp outbreaks has been delayed for more than 3 years in Europe and Asia (Sauteur et al., 2024). A long delay in epidemic resurgence is particularly alarming because it can allow for a build up of a large susceptible population, increasing the risk of a large outbreak as the infection resurges (Baker et al., 2020).

As Mp infections are beginning to increase rapidly in the US (Figure 1A), predicting the size of an impending outbreak is critical for public health agencies and decision makers. Here, we present a modeling analysis of Mp outbreaks in the US using data from 2015 onward and predictions for potential upcoming outbreaks and subsequent epidemic dynamics. We also explore counterfactual scenarios to tease apart factors that contributed to long delays in the resurgence of Mp outbreaks.

# 2 Methods

## 2.1 Data

We analyzed over 2.57 million BIOFIRE® Respiratory (RP1.7, RP2, and RP2.1) Panel (bioMérieux, Salt Lake City, Utah) multiplex PCR test results, 8678 of which had a positive detection of Mp (Poritz et al., 2011; Leber et al., 2018; Creager et al., 2020). These deidentified patient test results were captured from 127 US inpatient and outpatient facilities from January 1, 2015 to June 29, 2024 using BIOFIRE® Syndromic Trends, a cloud-

based pathogen surveillance network for BIOFIRE® instruments. Further details regarding the dataset and test result collection and interpretation methods have previously been published (Meyers et al., 2018). We also analyzed time-series data of influenza-like illnesses (ILIs), which were downloaded the FluView website (`https://gis.cdc.gov/grasp/fluview/fluportaldashboard.html`), and time-series data of Google Mobility for the US, which were taken from a previous publication (Park et al., 2024).

## 2.2 Incidence proxy

As discussed previously, test positivity can give a biased view of disease circulation patterns (Goldstein et al., 2011; Kissler et al., 2020; Park et al., 2024). Specifically, since test positivity in hospitals reflects prevalence of infection among individuals exhibiting respiratory symptoms, an increase (or decrease) in circulations of other respiratory diseases can cause test positivity of Mp infections to decrease (or increase). To mitigate this bias, we calculated an incidence proxy for Mp infections by multiplying weekly percentages of MP positives with weekly percentages of weighted ILIs. Limitations and assumptions to using this incidence proxy are discussed in Goldstein et al. (2011). Comparisons of three time series (Mp positivity, ILI positivity, and incidence proxy) are provided in Supplementary Figure S1.

## 2.3 Mathematical modeling of Mp outbreaks

To infer epidemic dynamics of Mp infections in the US, we fitted a seasonally-forced, deterministic Susceptible–Infectious–Recovered-Susceptible (SIRS) model to Mp time series data (Dushoff et al., 2004; Shaman et al., 2010). The SIRS model consists of three compartments, each representing the current infection status of an individual: Susceptible, Infected, and Recovered. We assumed a homogeneously mixed population, where infected individuals ($I$) transmit infection to susceptible individuals ($S$) at rate $\beta(t)$ and recover at rate $\gamma = 1/3$ weeks (Omori et al., 2015). Recovered individuals ($R$) were assumed to return to a susceptible state at rate $\nu$, which we estimated by fitting the model to data. Birth and death rates $\mu = 1/80$ years were assumed to be equal to fix the population size ($S + I + R = 10^6$). The model was discretized using the Euler scheme outlined in He et al. (2010) at a weekly

time scale $\Delta t = 1$ week:

$$\Delta S(t) = [1 - \exp(-(\beta(t)I(t) + \mu)\Delta t)]\, S(t - \Delta t) \tag{1}$$
$$N_{SI}(t) = \frac{\beta(t)I(t)\Delta S(t)}{\beta(t)I(t) + \mu} \tag{2}$$
$$\Delta I(t) = [1 - \exp(-(\gamma + \mu)\Delta t)]\, I(t - \Delta t) \tag{3}$$
$$N_{IR}(t) = \frac{\gamma \Delta I(t)}{\gamma + \mu} \tag{4}$$
$$\Delta R(t) = [1 - \exp(-(\nu + \mu)\Delta t)]\, R(t - \Delta t) \tag{5}$$
$$N_{RS}(t) = \frac{\nu \Delta R(t)}{\nu + \mu} \tag{6}$$
$$S(t) = S(t - \Delta t) + \mu S - \Delta S(t) + N_{RS}(t) \tag{7}$$
$$I(t) = I(t - \Delta t) - \Delta I(t) + N_{SI}(t) \tag{8}$$
$$R(t) = R(t - \Delta t) - \Delta R(t) + N_{IR}(t) \tag{9}$$
$$\tag{10}$$

where $\Delta X(t)$ represents the total number of individuals leaving the compartment $X$ at time $t$, and $N_{XY}(t)$ represents the number of individuals leaving the compartment $X$ to enter the compartment $Y$ at time $t$. We further calculated the incidence $C(t)$ by keeping track of the number of new infections in each week:

$$C(t) = N_{SI}(t), \tag{11}$$

which was fitted to estimated incidence proxy using a log-normal likelihood:

$$\log(\text{incidence proxy}) \sim \text{Normal}(\log(\rho C(t)), \sigma_{\text{obs}}), \tag{12}$$

where, $\rho$ represents the scaling factor and $\sigma_{\text{obs}}$ represents the residual standard deviation. Typically, either Poisson or negative binomial likelihoods are used to model discrete case counts; since incidence proxy is a continuous variable, we relied on the log-normal likelihood instead. For both $\rho$ and $\sigma_{\text{obs}}$, we used weakly informative half-normal priors:

$$\rho \sim \text{Half-Normal}(0, 2) \tag{13}$$
$$\sigma_{\text{obs}} \sim \text{Half-Normal}(0, 0.5). \tag{14}$$

In order to capture epidemic dynamics before and after NPIs were introduced, we extended the SIRS model by decomposing the transmission rate $\beta(t)$ into two separate terms: (1) a periodic term with a period of 1 year $\beta_{\text{seas}}(t)$ that captures seasonal transmission, reflecting epidemic peaks in summer and fall (Figure 1A) and (2) a non-periodic, time-varying term that captures changes in contact patterns after the introduction of COVID-19 NPIs in March, 2020 $\delta(t)$:

$$\beta(t) = \beta_{\text{seas}}(t)\delta(t), \tag{15}$$

where $\delta < 1$ corresponds to reduction in transmission due to NPI effects. The periodic term $\beta_{\text{seas}}(t)$ was modeled by estimating a weekly transmission rate for each of 52 weeks, which was modeled using cyclical, random-walk priors to allow for smoothing:

$$\beta_{\text{seas}}(t) \sim \text{Normal}(\beta_{\text{seas}}(t-1), \sigma) \qquad t = 2 \dots 52 \tag{16}$$

$$\beta_{\text{seas}}(1) \sim \text{Normal}(\beta_{\text{seas}}(52), \sigma) \tag{17}$$

To prevent estimating transmission rates that are unrealistically low or high, we also added a weakly informative prior:

$$\beta_{\text{seas}}(t) \sim \text{Normal}(1, 0.5). \tag{18}$$

A half-normal prior was used for the standard deviation of transmission smoothing $\sigma$:

$$\sigma \sim \text{Half-Normal}(0, 0.2). \tag{19}$$

The non-periodic term was modeled by estimating a separate $\delta$ for every four weeks with a normal prior centered around 1:

$$\delta(t) \sim \text{Normal}(1, 0.2). \tag{20}$$

We also used a weakly informative prior for the duration of immunity $\tau = 1/\nu$ to prevent extremely long or short duration of immunity:

$$\tau \sim \text{Normal}(300, 100). \tag{21}$$

Finally, we assumed a uniform prior for the initial proportion susceptible $S(0)$ and a half-normal prior for the initial proportion infected $I(0)$:

$$S(0) \sim \text{Unif}(0, 1) \tag{22}$$

$$I(0) \sim \text{Half-Normal}(0, 0.01) \tag{23}$$

The model was fitted using rstan (Carpenter et al., 2017; Stan Development Team, 2024) with 4 MCMC chains, each with 4000 iterations. Convergence was assessed based on the lack of warning signs from rstan, indicating: no divergent chains; no iterations exceeding maximum tree depth; sufficiently high Bayesian Fraction of Missing Information; sufficiently high effective samples sizes ($> 400$ for every parameter); and sufficiently low Rhat ($< 1.01$). The resulting posterior distribution was used to predict future Mp outbreaks by projecting the model forward.

As a sensitivity analysis, we also tried fitting the SIR model, which assumes that infection provides life-long immunity. The SIR model was implemented by setting the immune waning rate to zero, $\nu = 0$. This model was also fitted using the same priors and likelihood function with 4 MCMC chains, each with 6000 iterations.

### 2.4 Evaluating the impact of NPIs and waning immunity on the delays in re-emergence of Mp outbreak

It is currently unknown what factors contributed to long delays in re-emergence of the Mp outbreak. To evaluate the potential impact of NPIs and waning immunity on the timing of Mp re-emergence, we explored counterfactual scenarios by performing sensitivity analyses on how different assumptions about NPI effects and waning immunity can affect the timing of Mp outbreak resurgence; for simplicity, we tested the sensitivity of epidemic dynamics to each assumption independently (i.e., by varying one variable at a time) and did not explore their joint effects. First, the strength of NPIs were modified by taking the estimated fold changes in transmission $\delta - 1$ and scaling it by a factor of $\theta$ such that the resulting transmission rate corresponds to

$$\beta(t) = \beta_{\text{seas}}(t)[1 + \theta(\delta(t) - 1)]. \tag{24}$$

Second, the duration of NPIs were modified by assuming $\delta = 1$ after the end date $t_{\text{end}}$:

$$\beta(t) = \begin{cases} \beta_{\text{seas}}(t)\delta(t) & t < t_{\text{end}} \\ \beta_{\text{seas}}(t) & t \geq t_{\text{end}} \end{cases}. \tag{25}$$

We varied $t_{\text{end}}$ between 2020–2024. We also tested how the timing of NPI introduction, relative to the timing of multiannual cycles of Mp outbreak, by shifting $\delta(t)$ by 1–3 years to allow earlier introduction of NPIs. Finally, we varied the duration of immunity $1/\nu$ between 5–25 years to assess how waning immunity contributes to the timing of Mp outbreak resurgence. For illustration purposes, all other parameters are set to median values from the posterior throughout the analysis.

## 3 Results

**Mathematical modeling of past Mp epidemics.** The model reproduced the observed epidemic dynamics for Mp infections, including the seasonal and longer-term ($\approx$ 5 year) epidemic cycles before NPIs were introduced and the subsequent delayed resurgence of the epidemic (Figure 1A). To capture the response of Mp to the pandemic, the model required a strong reduction in transmission ($\delta(t) < 1$) in 2020 (Figure 1B). The model further estimated sustained reduction in transmission for 2021–2023 (Figure 1C). While we did not find a statistical correlation between the estimated changes in transmission and mean changes in Google mobility measures ($r$ = 0.14; 95% CI: -0.03, 0.30), the strength of correlation increased with lags, with strongest correlation occurring at a 4-week lag ($r$ = 0.36; 95% CI: 0.21–0.50; Supplementary Figure S2). The model demonstrated sinusoidal patterns in seasonal transmission—which is typical for respiratory infections—peaking around week 43 (Figure 1C). The model also estimated the mean duration of immunity to be 15.1 years (95% CI: 11.9 years–18.7 years). Comparisons between posterior and prior distributions are presented in Supplementary Figure S3. The SIR model gave nearly identical estimates for

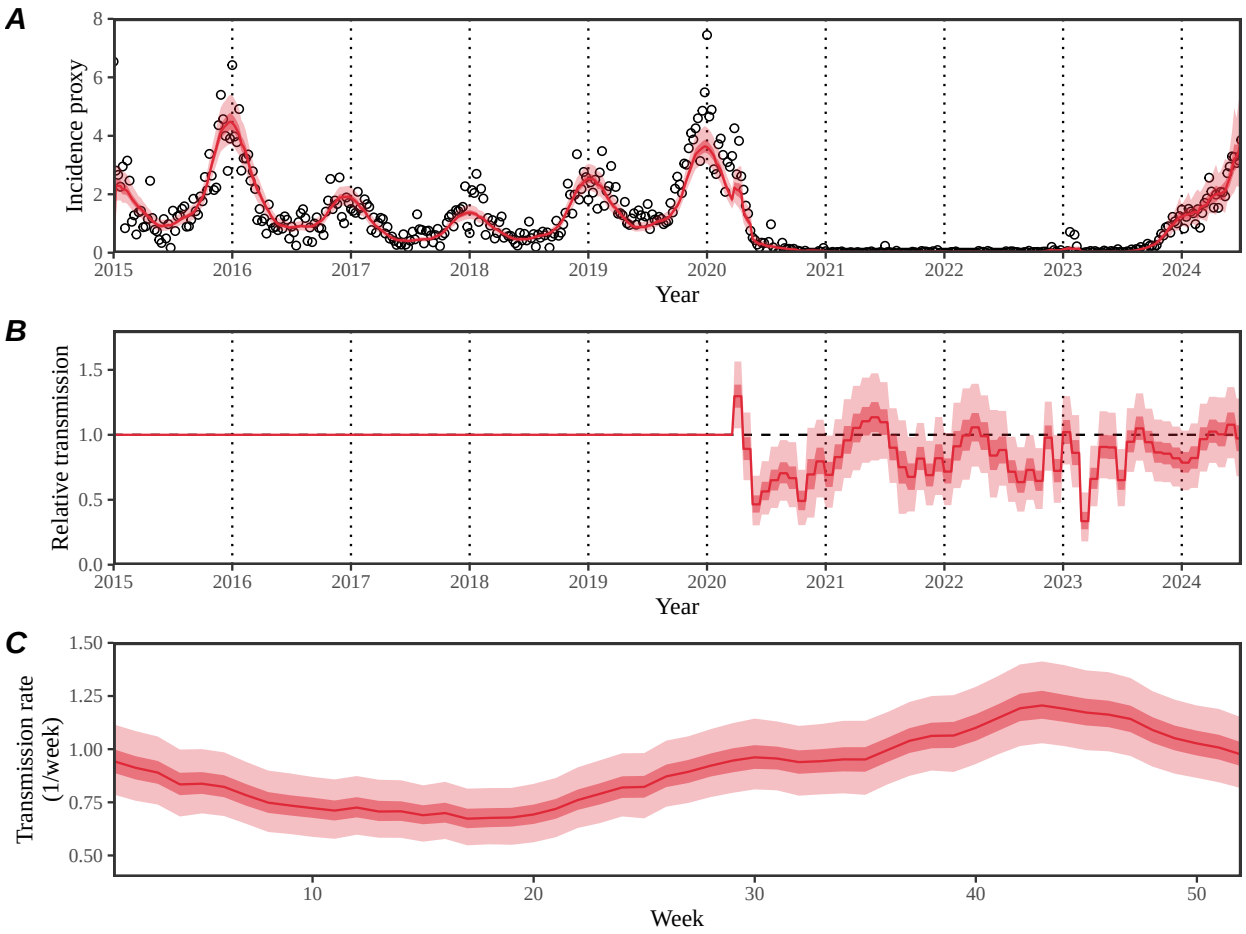


Figure 1: **Summary of model fits to Mycoplasma pneumoniae incidence proxy in the US, 2015–2024.** (A) Comparisons of observed (points) and fitted (line) trajectories of incidence proxy for Mp infections. (B) Estimated non-periodic, time-varying transmission term, representing relative transmission $\delta$ following the introduction of NPIs; for example, 0.5 corresponds to a 50% reduction in transmission. (C) Estimated periodic transmission term $\beta_{\text{seas}}(t)$, representing seasonal transmission rate. Red lines and shaded regions represent the estimated posterior median and corresponding 95% and 50% credible intervals.

the NPI effects and transmission rates but underestimated the peak of the 2015 outbreak, providing support for the SIRS model (Supplementary Figure S4).

**Prediction of future Mp outbreaks.** In line with other acute, partially immunizing respiratory pathogens (Baker et al., 2020), the model predicted a large build-up of the susceptible pool during the NPI period (Figure 2A). This increase in susceptible individuals could lead to a large Mp outbreak, which appears to have begun since the beginning of 2024 (Figure 1A); the model forecasted that the epidemic would peak around the second half of 2024 and start to decline towards the end of 2024 (Figure 2B), reflecting a decrease in transmission rate in winter (Figure 1C). The peak incidence during this outbreak is estimated

to be 4.9 (95% CI: 4.0–6.0) times larger than previous peaks. The model further predicted that the outbreak beginning in 2024 would cause a large depletion of the susceptible pool (Figure 2A), which would lead to another delayed outbreak after several years (Figure 2B).

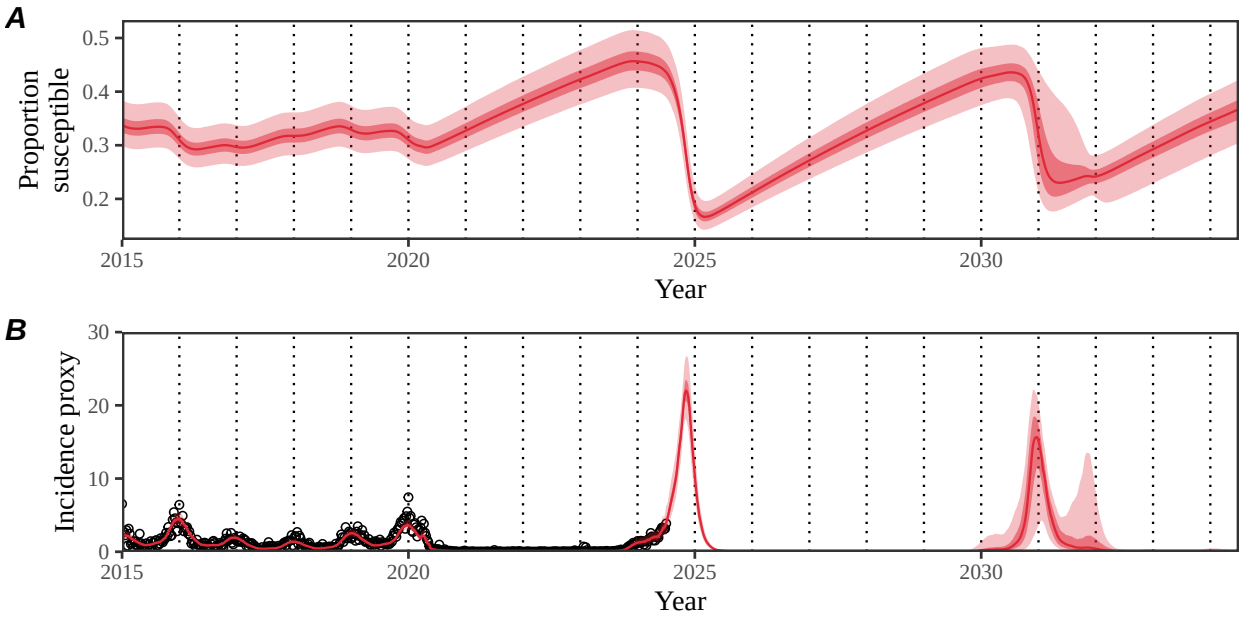


Figure 2: **Predictions of future Mycoplasma pneumoniae outbreaks.** (A) Predicted changes in the proportion of susceptible individuals. (B) Predicted changes in weekly incidence proxy for Mp infections. Red lines and shaded regions represent the estimated posterior median and corresponding 95% and 50% credible intervals. Points represent the observed incidence proxy.

**Impact of NPI pattern and waning immunity on the timing of Mp outbreak resurgence.** The model predicted that a strong reduction in transmission due to NPIs is critical to explaining long delays in the Mp outbreak resurgence. A smaller reduction in transmission (Figure 3A) would have led to more persistent epidemics as well as earlier resurgence of Mp outbreaks (Figure 3B). Interestingly, the model still predicted a large outbreak in 2023 even when we assumed that NPI effects were 50–75% weaker than what we originally estimated, demonstrating the risk of a susceptible build up. Similarly, assuming shorter duration of NPIs (Figure 3C) led to earlier resurgence (Figure 3D). However, even if transmission rates were to return to pre-pandemic values by the end of 2020, the model predicted that the resurgence would not be observed until the middle of 2022 (Figure 3D). We also find that the timing of NPIs, relative to the timing of relative to the timing of multiannual cycles of Mp outbreak, can affect the timing of resurgence (Supplementary Figure S5). Specifically, when NPIs are introduced after a major outbreak, a large susceptible depletion caused by the major outbreak can drive a longer delay until the resurgence. Instead, if NPIs were introduced 1 or 2 years earlier (thus before the major outbreak that occurred in the winter of 2019), the duration of honeymoon period would have been shorter. Finally,

we found that the duration of immunity was also a key factor in determining the delays in Mp outbreak resurgences (Figure 3E): faster waning of immunity would have caused a faster build up of the susceptible pool, leading to an earlier Mp outbreak.

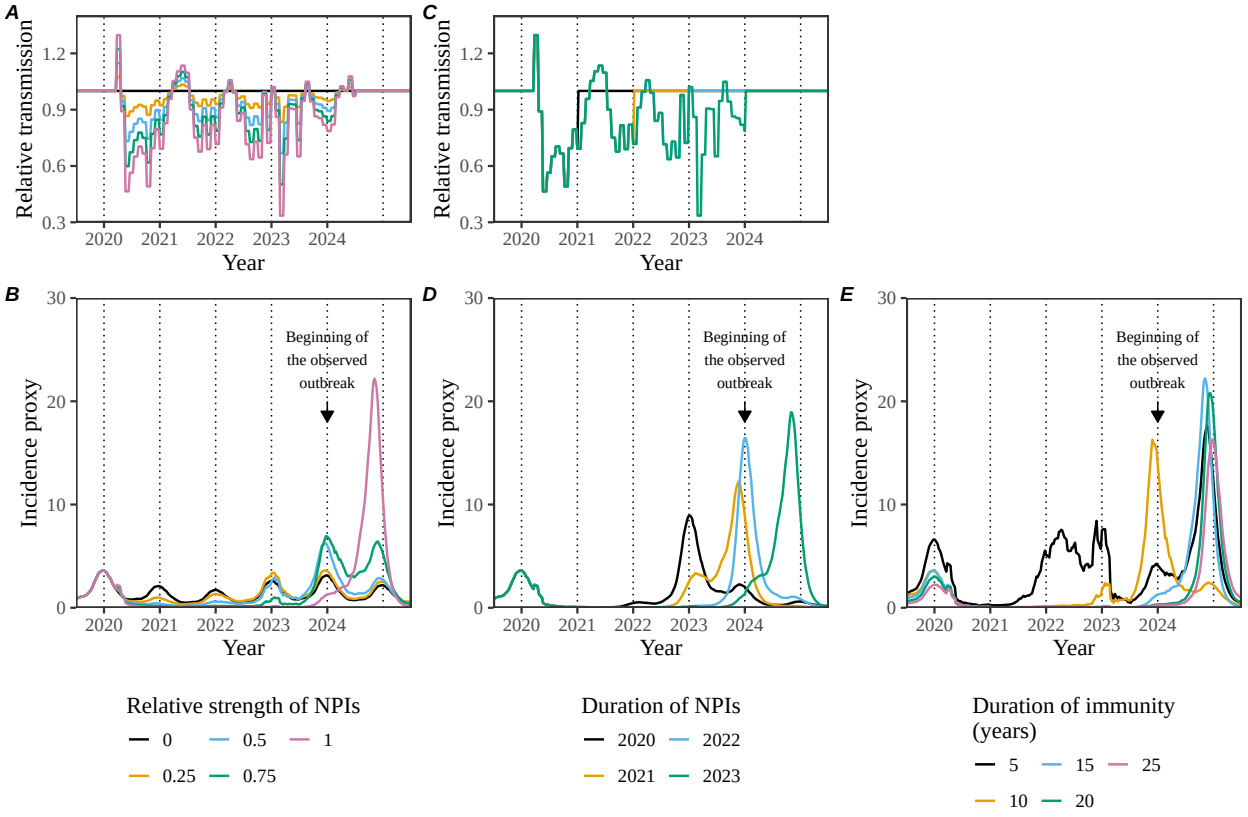


Figure 3: **Impact of strength and duration of NPIs on the timing of Mp outbreak resurgence.** (A, C) Assumed values for the relative transmission term $\delta$ following the introduction of NPIs by varying the strength (A) and duration (C) of NPIs. (B, D) Resulting epidemic dynamics across different assumptions about NPIs. (E) Resulting epidemic dynamics across different assumptions about the duration of immunity. The arrows indicate the beginning of the observed outbreak as a reference.

# 4 Discussion

In this study, we investigated the impact of NPIs on future Mp outbreaks in the US. By fitting a mathematical model to syndromic surveillance data, we predicted that a large Mp outbreak is imminent with a peak expected before the end of 2024. The upcoming outbreak is expected to be much larger than past outbreaks and may last until the end of 2025; note, however, that there is currently substantial uncertainty associated with longer-term dynamics, including the duration of 2024–2025 outbreak and the timing of the subsequent

outbreaks. By the beginning of 2024, we could already observe what seems to be the beginning of this outbreak with an increasing rate of Mp detections throughout May and June 2024. This prediction should alert clinicians and health care systems to be prepared for an increase in cases of pneumonia and potentially more rare presentations of Mp, such as reactive infectious mucocutaneous eruption (RIME) and encephalitis.

Our analysis highlighted the importance of a strong reduction in transmission in explaining the delayed resurgence of Mp outbreaks. Specifically, we estimated $\approx 50\%$ reduction in transmission in 2020, which is considerably larger than the reduction in transmission estimated for other respiratory pathogens. For example, Baker et al. (2020) estimated a 20% reduction in RSV transmission in the beginning of 2020. Future studies should explore whether the epidemiology and life history of Mp infections cause its transmission to be more susceptible to behavioral changes. Our analyses also suggest that the duration of NPIs, relative timing of NPIs, and the duration of immunity against MP infections also contributed to the long delays in resurgence.

There are several limitations to our study. The dataset inherently contains a subset of the US population that has presented to facilities that utilizes the BIOFIRE® Respiratory Panel and participates in the BIOFIRE® Syndromic Trends network. As with many surveillance network data, this assumes inherent selection bias for less healthy individuals than the general population, therefore introducing the limitation of representativeness of the dataset. Additionally, due to the nature of deidentified data collection within the dataset, we are not able to conduct analyses based on patient or facility characteristics or account for variability in diagnostic testing algorithms between facilities. However, this dataset has evidenced correlation with other surveillance sources, reducing concern regarding representativeness and generalizability (Meyers et al., 2018).

We did not account for heterogeneity in Mp dynamics across states as the quantity of data did not allow for reliable model-fitting at a regional scale. We did not include age structure in the model as it would require more data. We also did not account for Mp strain dynamics, which have been hypothesized as another major driver of epidemic cycles (Kenri et al., 2008; Zhang et al., 2019). Finally, our estimate of NPI effects need to be interpreted with care, especially during a period with very little case data; in particular, our estimates of NPI effects will try to capture all other mechanisms that affect infection and transmission, not just those directly caused by NPIs. Despite these limitations, our prediction that a build up of a susceptible pool over the past 4 years will cause a large Mp outbreak is likely qualitatively robust.

So far, there have been limited modeling studies analyzing epidemic dynamics of Mp infections (Omori et al., 2015; Zhang et al., 2019). Our study reinforces recent work on the importance of understanding susceptible dynamics to predict the impact of perturbations to transmission (Baker et al., 2020; Park et al., 2024). As such, our analysis underlines the importance of serological surveillance data to capture the build up of the susceptible pool to foresee future outbreaks (Mina et al., 2020; Nguyen-Tran et al., 2022). Our study also underlines the potential of BIOFIRE® Syndromic Trends network as a powerful surveillance measure (Park et al., 2021).

## Data availability

All code is stored in a publicly available GitHub repository (`https://github.com/parksw3/mycoplasma_pred`).


## Funding

S.W.P. is a Peter and Carmen Lucia Buck Foundation Awardee of the Life Sciences Research Foundation. B.F.N. receives funding from Carlsberg Foundation (grant no. CF23-0173). K.M. receives funding as Principal Investigator of the NIAID Vaccine Research Center PREMISE EV-D68 Pilot Study.


## Conflict of interest

B.N. and S.L. are employees of bioMérieux. bioMérieux markets the BIOFIRE® System and Syndromic Trends. BIOMÉRIEUX, the BIOMÉRIEUX logo, BIOFIRE, FILMARRAY are used, pending and/or registered trademarks belonging to bioMérieux or one of its subsidiaries. L.A's institution has received grant funding from Pfizer Inc. for an unrelated study. S.D. receives grant support from BIOFIRE Diagnostics, DelveBio, and Karius; he is also a consultant for BIOFIRE Diagnostics, DelveBio, and Karius.

# Supplementary Figures

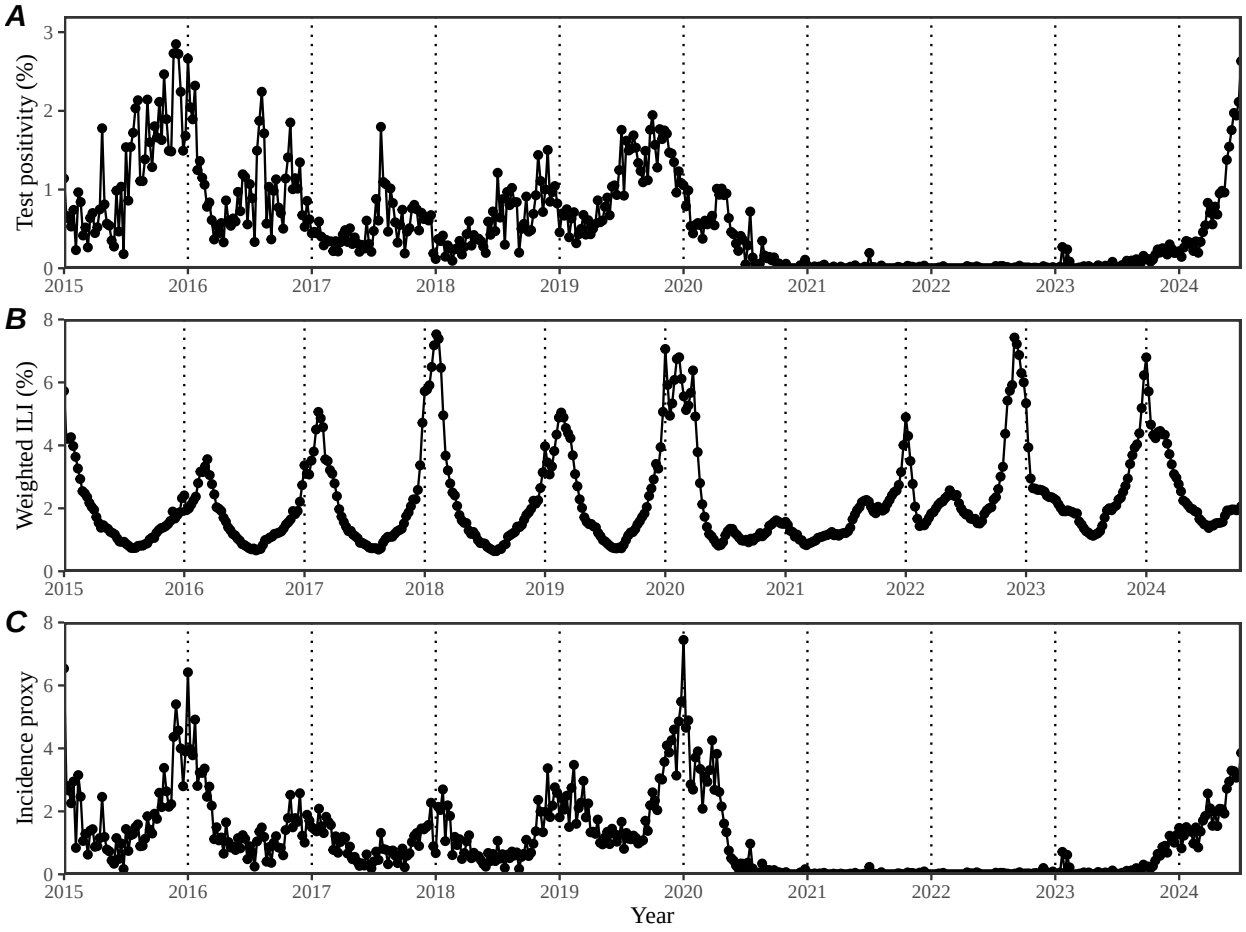


Figure S1: **Comparisons of time series data.** (A) Weekly percent positivity of Mp infections BIOFIRE® Respiratory Panel in the US. (B) Weekly percent positivity of outpatient visits for ILI in the US. (C) Estimated weekly incidence proxy.

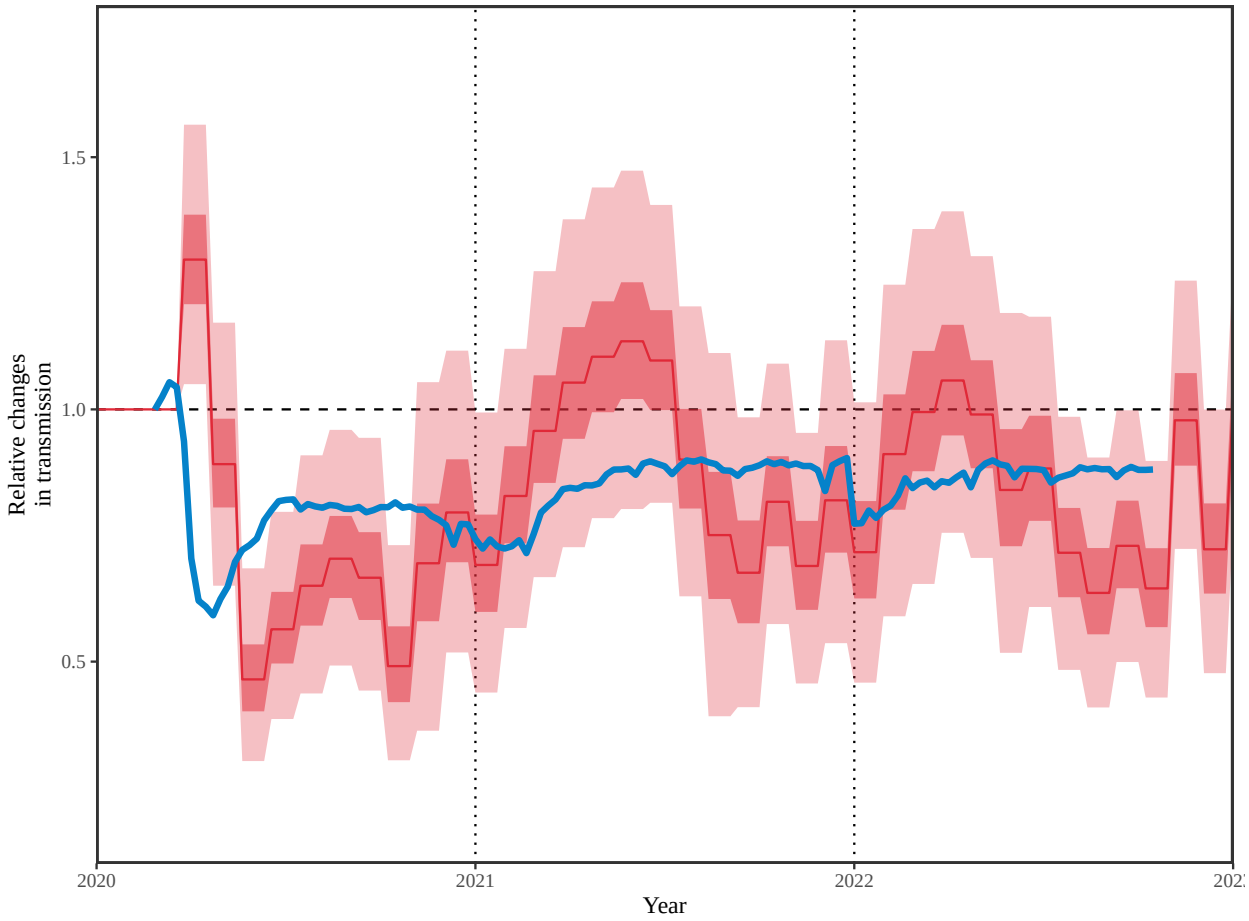


Figure S2: **Comparisons of estimated changes in transmission (red) and mean Google mobility measures (blue).** Mean mobility was calculated by taking the average mobility across four categories: retail & recreation, grocery & pharmacy, transit stations, and workplaces (Park et al., 2024).

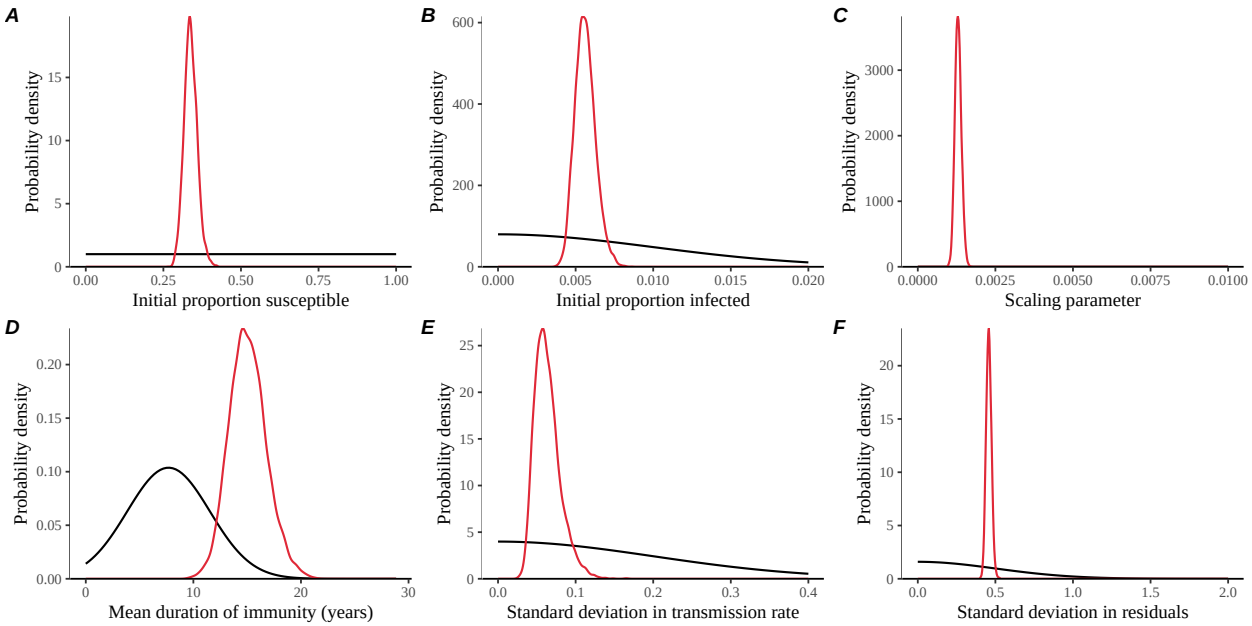


Figure S3: **Comparisons between posterior and prior distributions.** Black lines represent prior distributions. Red lines represent posterior distributions. Posterior distributions for the seasonal transmission rate and NPI effects are presented in Figure 1. Note that the prior distribution for the scaling parameter is not visible in panel C because the assumed distribution is much wider (a half normal with a mean of 0 and standard deviation of 2) and therefore has much lower densities.

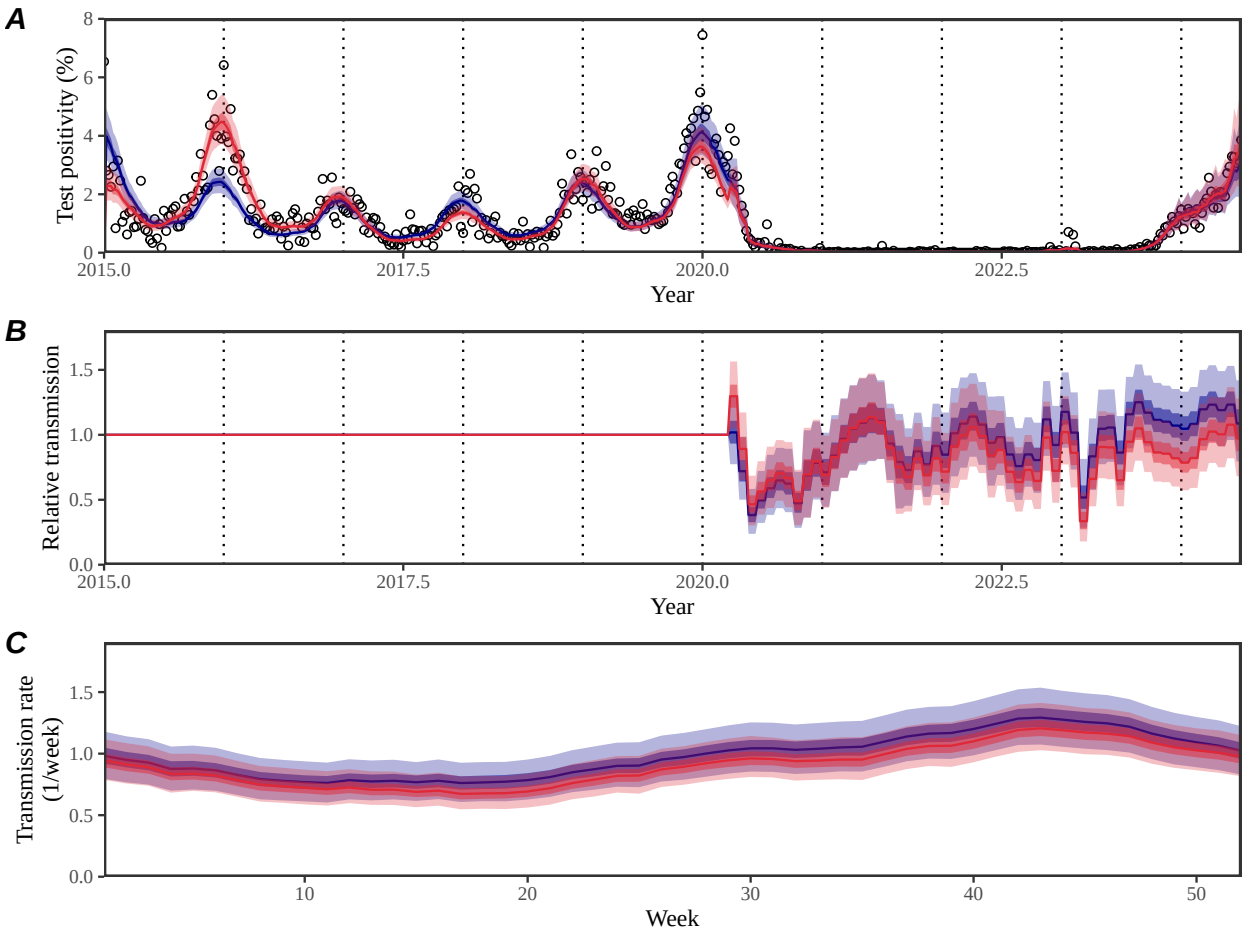


Figure S4: **Comparisons of SIRS (red) and SIR (blue) model fits to Mycoplasma pneumoniae positivity in the US, 2015–2024.** (A) Comparisons of observed (points) and fitted (line) changes in weekly test positivity for Mp infections. (B) Estimated non-periodic, time-varying transmission term, representing relative transmission $\delta$ following the introduction of NPIs. These changes are relative to the seasonal transmission rate shown in panel C; for example, 0.5 corresponds to a 50% reduction in transmission. (C) Estimated periodic transmission term $\beta_{\text{seas}}(t)$, representing seasonal transmission rate. Lines and shaded regions represent the estimated posterior median and corresponding 95% and 50% credible intervals.

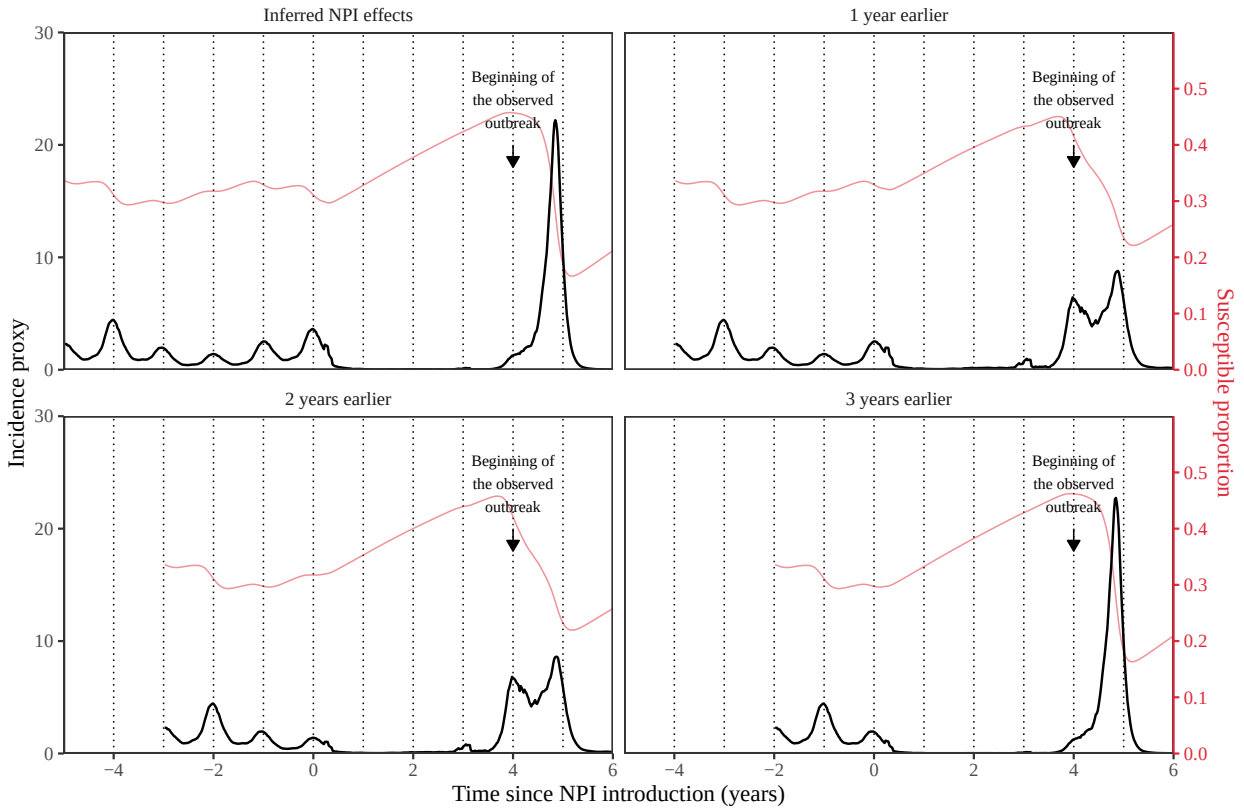


Figure S5: **Impact of timing of NPI introduction, relative to the timing of the multiannaul cycles of Mp outbreaks.** Sensitivity analyses were performed by shifting the estimated $\delta$ by 1–3 years to explore counterfactual scenarios that allow earlier introduction of NPIs. The first panel (inferred NPI effects) represent our main predictions (shown in Figure 2 in the main text) following the observed epidemic. All other panels represent counterfactual simulations. Black lines represent the predicted incidence proxy. Red lines represent the predicted susceptible proportion.

# References


Bajantri, B., S. Venkatram, and G. Diaz-Fuentes (2018). Mycoplasma pneumoniae: a potentially severe infection. *Journal of clinical medicine research 10*(7), 535.

Baker, R. E., S. W. Park, W. Yang, G. A. Vecchi, C. J. E. Metcalf, and B. T. Grenfell (2020). The impact of COVID-19 nonpharmaceutical interventions on the future dynamics of endemic infections. *Proceedings of the National Academy of Sciences 117*(48), 30547–30553.

Boyanton Jr, B. L., R. A. Frenner, A. Ingold, L. Ambroggio, and J. L. Kennedy (2024). SARS-CoV-2 pandemic non-pharmacologic interventions temporally associated with reduced pediatric infections due to Mycoplasma pneumoniae and co-infecting respiratory viruses in Arkansas. *Microbiology Spectrum 12*(4), e02908–23.

Brown, R. J., P. Nguipdop-Djomo, H. Zhao, E. Stanford, O. B. Spiller, and V. J. Chalker (2016). Mycoplasma pneumoniae epidemiology in England and Wales: a national perspective. *Frontiers in microbiology 7*, 157.

Carpenter, B., A. Gelman, M. D. Hoffman, D. Lee, B. Goodrich, M. Betancourt, M. A. Brubaker, J. Guo, P. Li, and A. Riddell (2017). Stan: A probabilistic programming language. *Journal of statistical software 76*.

Creager, H. M., B. Cabrera, A. Schnaubelt, J. L. Cox, A. M. Cushman-Vokoun, S. M. Shakir, K. D. Tardif, M.-L. Huang, K. R. Jerome, A. L. Greninger, et al. (2020). Clinical evaluation of the BioFire® Respiratory Panel 2.1 and detection of SARS-CoV-2. *Journal of Clinical Virology 129*, 104538.

Dushoff, J., J. B. Plotkin, S. A. Levin, and D. J. Earn (2004). Dynamical resonance can account for seasonality of influenza epidemics. *Proceedings of the National Academy of Sciences 101*(48), 16915–16916.

Earn, D. J., P. Rohani, B. M. Bolker, and B. T. Grenfell (2000). A simple model for complex dynamical transitions in epidemics. *science 287*(5453), 667–670.

Goldstein, E., S. Cobey, S. Takahashi, J. C. Miller, and M. Lipsitch (2011). Predicting the epidemic sizes of influenza A/H1N1, A/H3N2, and B: a statistical method. *PLoS medicine 8*(7), e1001051.

He, D., E. L. Ionides, and A. A. King (2010). Plug-and-play inference for disease dynamics: measles in large and small populations as a case study. *Journal of the Royal Society Interface 7*(43), 271–283.

Jain, S., W. H. Self, R. G. Wunderink, S. Fakhran, R. Balk, A. M. Bramley, C. Reed, C. G. Grijalva, E. J. Anderson, D. M. Courtney, et al. (2015). Community-acquired pneumonia requiring hospitalization among US adults. *New England Journal of Medicine 373*(5), 415–427.

Jain, S., D. J. Williams, S. R. Arnold, K. Ampofo, A. M. Bramley, C. Reed, C. Stockmann, E. J. Anderson, C. G. Grijalva, W. H. Self, et al. (2015). Community-acquired pneumonia requiring hospitalization among US children. *New England Journal of Medicine 372*(9), 835–845.

Keeling, M. J., P. Rohani, and B. T. Grenfell (2001). Seasonally forced disease dynamics explored as switching between attractors. *Physica D: Nonlinear Phenomena 148*(3-4), 317–335.

Kenri, T., N. Okazaki, T. Yamazaki, M. Narita, K. Izumikawa, M. Matsuoka, S. Suzuki, A. Horino, and T. Sasaki (2008). Genotyping analysis of Mycoplasma pneumoniae clinical strains in Japan between 1995 and 2005: type shift phenomenon of M. pneumoniae clinical strains. *Journal of medical microbiology 57*(4), 469–475.

Kim, J. W., H. K. Seo, E. G. Yoo, S. J. Park, S. H. Yoon, H. Y. Jung, and M. Y. Han (2009). Mycoplasma pneumoniae pneumonia in Korean children, from 1979 to 2006-a meta-analysis. *Clinical and Experimental Pediatrics 52*(3), 315–323.

Kissler, S. M., C. Tedijanto, E. Goldstein, Y. H. Grad, and M. Lipsitch (2020). Projecting the transmission dynamics of SARS-CoV-2 through the postpandemic period. *Science 368*(6493), 860–868.

Leber, A. L., K. Everhart, J. A. Daly, A. Hopper, A. Harrington, P. Schreckenberger, K. McKinley, M. Jones, K. Holmberg, and B. Kensinger (2018). Multicenter evaluation of BioFire FilmArray respiratory panel 2 for detection of viruses and bacteria in nasopharyngeal swab samples. *Journal of Clinical Microbiology 56*(6), 10–1128.

Meyers, L., C. C. Ginocchio, A. N. Faucett, F. S. Nolte, P. H. Gesteland, A. Leber, D. Janowiak, V. Donovan, J. D. Bard, S. Spitzer, et al. (2018). Automated real-time collection of pathogen-specific diagnostic data: syndromic infectious disease epidemiology. *JMIR public health and surveillance 4*(3), e9876.

Mina, M. J., C. J. E. Metcalf, A. B. McDermott, D. C. Douek, J. Farrar, and B. T. Grenfell (2020). A Global lmmunological Observatory to meet a time of pandemics. *Elife 9*, e58989.

Nguyen-Tran, H., S. W. Park, K. Messacar, S. R. Dominguez, M. R. Vogt, S. Permar, P. Permaul, M. Hernandez, D. C. Douek, A. B. McDermott, et al. (2022). Enterovirus D68: a test case for the use of immunological surveillance to develop tools to mitigate the pandemic potential of emerging pathogens. *The Lancet Microbe 3*(2), e83–e85.

Olson, D., L. K. F. Watkins, A. Demirjian, X. Lin, C. C. Robinson, K. Pretty, A. J. Benitez, J. M. Winchell, M. H. Diaz, L. A. Miller, et al. (2015). Outbreak of Mycoplasma pneumoniae–associated Stevens-Johnson syndrome. *Pediatrics 136*(2), e386–e394.

Omori, R., Y. Nakata, H. L. Tessmer, S. Suzuki, and K. Shibayama (2015). The determinant of periodicity in Mycoplasma pneumoniae incidence: an insight from mathematical modelling. *Scientific reports 5*(1), 14473.

Park, S. W., K. Messacar, D. C. Douek, A. B. Spaulding, C. J. E. Metcalf, and B. T. Grenfell (2024). Predicting the impact of COVID-19 non-pharmaceutical intervention on short-and medium-term dynamics of enterovirus D68 in the US. *Epidemics 46*, 100736.

Park, S. W., M. Pons-Salort, K. Messacar, C. Cook, L. Meyers, J. Farrar, and B. T. Grenfell (2021). Epidemiological dynamics of enterovirus D68 in the United States and implications for acute flaccid myelitis. *Science Translational Medicine 13*(584), eabd2400.

Pereyre, S., J. Goret, and C. Bébéar (2016). Mycoplasma pneumoniae: current knowledge on macrolide resistance and treatment. *Frontiers in microbiology 7*, 974.

Poritz, M. A., A. J. Blaschke, C. L. Byington, L. Allen, K. Nilsson, D. E. Jones, S. A. Thatcher, T. Robbins, B. Lingenfelter, E. Amiott, et al. (2011). FilmArray, an automated nested multiplex PCR system for multi-pathogen detection: development and application to respiratory tract infection. *PloS one 6*(10), e26047.

Sauteur, P. M. M., M. L. Beeton, S. Pereyre, C. Bébéar, M. Gardette, N. Hénin, N. Wagner, A. Fischer, A. Vitale, B. Lemaire, et al. (2024). Mycoplasma pneumoniae: delayed re-emergence after COVID-19 pandemic restrictions. *The Lancet Microbe 5*(2), e100–e101.

Shaman, J., V. E. Pitzer, C. Viboud, B. T. Grenfell, and M. Lipsitch (2010). Absolute humidity and the seasonal onset of influenza in the continental United States. *PLoS biology 8*(2), e1000316.

Stan Development Team (2024). RStan: the R interface to Stan. R package version 2.32.6.

Waites, K. B. and D. F. Talkington (2004). Mycoplasma pneumoniae and its role as a human pathogen. *Clinical microbiology reviews 17*(4), 697–728.

Walter, N. D., G. B. Grant, U. Bandy, N. E. Alexander, J. M. Winchell, H. T. Jordan, J. J. Sejvar, L. A. Hicks, D. R. Gifford, N. T. Alexander, et al. (2008). Community outbreak of Mycoplasma pneumoniae infection: school-based cluster of neurologic disease associated with household transmission of respiratory illness. *Journal of Infectious Diseases 198*(9), 1365–1374.

Zhang, X.-S., H. Zhao, E. Vynnycky, and V. Chalker (2019). Positively interacting strains that co-circulate within a network structured population induce cycling epidemics of Mycoplasma pneumoniae. *Scientific reports 9*(1), 541.